

# One-pot synthesis of reverse type-I $\text{In}_2\text{O}_3@ \text{In}_2\text{S}_3$ core-shell nanoparticles†

Zhaoyong Sun,<sup>a</sup> Amar Kumbhar,<sup>b</sup> Kai Sun,<sup>c</sup> Qingsheng Liu<sup>d</sup> and Jiye Fang<sup>\*ae</sup>

Received (in Berkeley, CA, USA) 13th December 2007, Accepted 1st March 2008

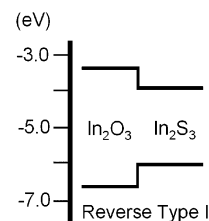
First published as an Advance Article on the web 18th March 2008

DOI: 10.1039/b719176f

**A novel method to one-pot-synthesize high-quality  $\text{In}_2\text{O}_3@ \text{In}_2\text{S}_3$  core-shell nanoparticles, consisting of a step of reducing  $\text{In}_2\text{O}_3$  core surface into a layer of active indium metal in high-temperature organic solution and a step of converting this layer to  $\text{In}_2\text{S}_3$  using  $\text{CS}_2$ , has been developed.**

Although study of semiconductor core-shell nanoparticles (NPs) has attracted increasing scientific and technological interest due to the ability to fine-tune their properties,<sup>1–4</sup> the most extensive syntheses were focused on type-I core-shell NPs,<sup>5–8</sup> in which a wide bandgap material is coated onto the core of a narrow bandgap material. There have been relatively rare reports concerning the preparation of reverse type-I core-shell NPs,<sup>9</sup> in which a narrow bandgap material is overgrown on the core of a wide bandgap material and unique characteristic may be observed. Indium oxide ( $\text{In}_2\text{O}_3$ ), widely used in solar cells and optoelectronic devices,<sup>10</sup> is a direct wide bandgap and photostable<sup>11</sup> material ( $\sim 3.6$  eV),<sup>12</sup> whereas indium sulfide ( $\text{In}_2\text{S}_3$ ) is a visible-light-sensitive semiconductor with a bandgap as narrow as  $\sim 2.00\text{--}2.30$  eV (bulk)<sup>13–15</sup> (see Scheme 1). It has already demonstrated that the  $\text{In}_2\text{O}_3@ \text{In}_2\text{S}_3$  core-shell structure as electrodes on micrometer-level could generate high anodic photocurrent.<sup>11,16</sup> Here we demonstrate a feasible and simple approach to one-pot-synthesize high-quality  $\text{In}_2\text{O}_3@ \text{In}_2\text{S}_3$  core-shell particles on the nanometer level.

The preparation of  $\text{In}_2\text{O}_3@ \text{In}_2\text{S}_3$  core-shell NPs involves an initial synthesis of  $\text{In}_2\text{O}_3$  nanocrystals (NCs), a subsequent reduction of the surface of  $\text{In}_2\text{O}_3$  NCs, and a further sulfidization to form  $\text{In}_2\text{S}_3$  shells. It has been reported that nano-scale  $\text{In}_2\text{O}_3$  can be prepared through various reaction routes, such as oxidation by trimethylamine oxide (TMNO),<sup>10</sup> aminolysis on the InP surface by oleylamine,<sup>8</sup> and alcoholysis in organic solvent.<sup>17</sup> In consideration of the next reduction procedure, we modified our previous strategy of  $\text{In}_2\text{O}_3$  synthesis<sup>10</sup> by altering



**Scheme 1** Bandgap energy levels in  $\text{In}_2\text{O}_3$  and  $\text{In}_2\text{S}_3$ .

the heating rate and skipping the oxidizing step in which TMNO was involved. Generally, TMNO could assist in refining the morphology of  $\text{In}_2\text{O}_3$  NCs, such as octahedral shape, which is obviously not a significant consideration in the current approach.

In a typical experiment, 0.20 mmol of indium acetate (99.99%), 0.60 mL of oleic acid (90%) and 0.80 mL of oleylamine (70%, all chemicals were from Aldrich without further purification) were combined with 5.0 mL of octadecene in a three-necked round-bottomed flask equipped with a condenser in a fume hood. Standard air-free techniques were used. The vigorously stirred mixture was heated to 120 °C under an argon purge. This temperature was held for 20 min and then rapidly raised to 320 °C at a rate of 15 °C min<sup>-1</sup> and the system was vigorously agitated and refluxed for an additional 40 min under an argon stream. During this reflux period, the transparent yellow mixture became a slurry at  $\sim 300$  °C, subsequently changed to clear yellow again in  $\sim 1$  min, and finally turned light brown. When the mixture was cooled to 140 °C, 1 mL of the colloidal  $\text{In}_2\text{O}_3$  suspension was collected using a glass syringe with a long needle into 30 mL of anhydrous ethanol<sup>18</sup> followed by centrifugation and re-dispersion into a certain amount of anhydrous hexane as a “core” sample for the purpose of comparison. It has recently been reported that  $\text{WO}_x$  nanorods could be converted into  $\text{WS}_2$  nanosheets using  $\text{CS}_2$  at high temperature.<sup>19</sup> To achieve core-shell NPs in our system, we performed a reduction and a subsequent sulfidization in the same flask. Typically, 0.5 mL of freshly prepared superhydride solution in dioctyl ether<sup>20</sup> (1.0 M) was injected into the rest of the reaction system at 140 °C under argon protection. After agitation for 30 min, 0.5 mL of  $\text{CS}_2$  solution in toluene (0.4 M) was further injected into the flask and the color of the solution immediately turned orange. The system was continuously stirred for 20 min, followed by an additional 35 min vigorous agitation when the temperature was increased to 250 °C at a rate of 5.5 °C min<sup>-1</sup>. In order to trap the excess  $\text{CS}_2$  which is highly toxic, the exhaust stream from the reaction system was introduced into a bottle containing excess ethanol before it was released into the fume hood. The resultant colloids were

<sup>a</sup> Department of Chemistry, State University of New York at Binghamton, Binghamton, NY 13902, USA

<sup>b</sup> Electron Microscope Facility, Clemson University, Anderson, SC 29625, USA

<sup>c</sup> Electron Microbeam Analysis Laboratory, University of Michigan, Ann Arbor, MI 48109, USA

<sup>d</sup> Department of Chemistry, Texas A&M University, College Station, TX 77842, USA

<sup>e</sup> Multidisciplinary Program in Materials Science & Engineering, State University of New York at Binghamton, Binghamton, NY 13902, USA. E-mail: jfang@binghamton.edu; Fax: +1 607 777 4478; Tel: +1 607 777 3752

† Electronic supplementary information (ESI) available: TEM of  $\text{In}_2\text{O}_3$  NCs; TEM, HRTEM and PL of  $\text{In}_2\text{O}_3@ \text{In}_2\text{S}_3$  core-shell NPs. See DOI: 10.1039/b719176f

cooled to room temperature and isolated by adding anhydrous ethanol, and collected by centrifugation. The resulting white-grey precipitate could be partially re-dispersed in anhydrous hexane, forming a suspension of  $\text{In}_2\text{O}_3@ \text{In}_2\text{S}_3$  core-shell NPs with a very narrow distribution of particle size. The capability of dispersion in hexane could be enhanced by adding a drop of oleic acid.

The morphology and phase structure of these core-shell NPs were evaluated using transmission electron microscopes (TEM) (Hitachi 7600 & 9500, HD 2000) and an X-ray diffractometer (XRD) (PANalytical X-pert system), respectively. A typical TEM image of  $\text{In}_2\text{O}_3$  NCs in low magnification is shown in Fig. 1A, showing that the  $\text{In}_2\text{O}_3$  NCs possess an average diameter of  $\sim 10$  nm and a short-range, hexagonal order of self-assembled pattern. Fig. 1B shows the structure of  $\text{In}_2\text{O}_3@ \text{In}_2\text{S}_3$  core-shell NPs in low magnification, revealing that the average diameter of the entire core-shell NPs is  $\sim 16$

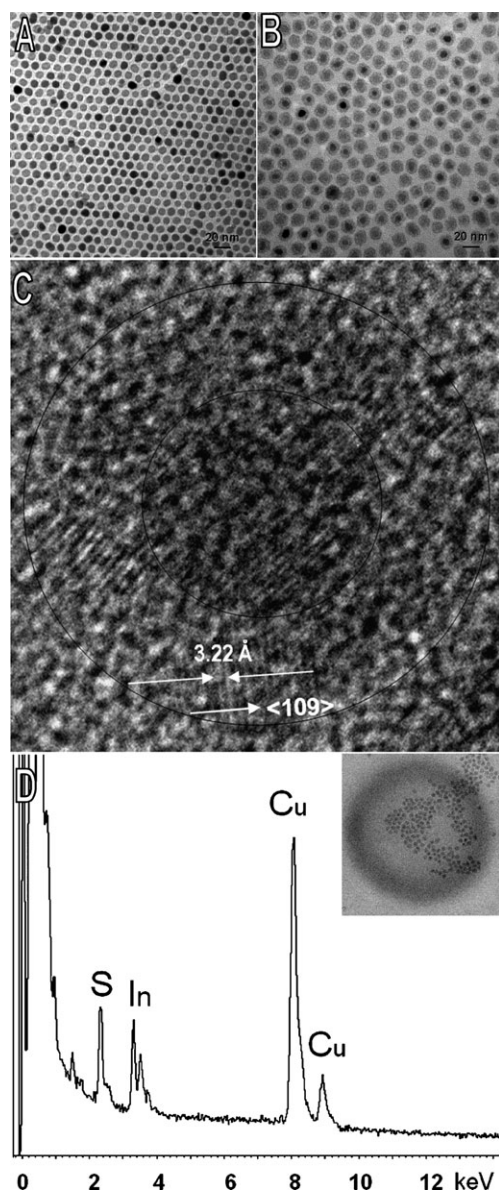


**Fig. 1** (A) TEM image of  $\text{In}_2\text{O}_3$  core NCs; (B) TEM image of  $\text{In}_2\text{O}_3@ \text{In}_2\text{S}_3$  core-shell NPs; (C) HRTEM image of  $\text{In}_2\text{O}_3@ \text{In}_2\text{S}_3$  NPs; and (D) EDS of  $\text{In}_2\text{O}_3@ \text{In}_2\text{S}_3$  NPs; the inset shows the selected NPs.

nm, which is broken down into a  $\sim 8$  nm diameter of the  $\text{In}_2\text{O}_3$  cores and a  $\sim 4$  nm thickness of the  $\text{In}_2\text{S}_3$  shells (also see Fig. S1 in ESI<sup>†</sup>). This observation also demonstrates “shrinkage” of the  $\text{In}_2\text{O}_3$  NCs from  $\sim 10$  to  $\sim 8$  nm in diameter due to the surface reduction by superhydride, indicating that the  $\text{In}_2\text{O}_3$  surface of  $\sim 1$  nm thickness was reduced to highly active In and subsequently converted to a  $\text{In}_2\text{S}_3$  layer of thickness  $\sim 4$  nm. In this shell-formation process, highly active elemental sulfur was freshly provided by the thermal decomposition of  $\text{CS}_2$ . As displayed in Fig. 1C, the core-shell structure can be verified by the high resolution TEM (HRTEM) image, demonstrating well-developed lattice structures on both core and shell portions (also see Fig. S1c in ESI<sup>†</sup>). The lattice pattern of  $\text{In}_2\text{O}_3$  core is well-resolved and shows a single crystalline structure; whereas the highly crystalline shell can be further identified as  $\text{In}_2\text{S}_3$  based on the measured lattice distance of  $3.22 \text{ \AA}$  which is considerably consistent with that ( $d = 3.25 \text{ \AA}$ ) of tetragonal  $\text{In}_2\text{S}_3$  lattice planes  $\{109\}$ . Fig. 1D is the energy dispersive X-ray spectrum (EDS), revealing that the S constituent of the coating shell occupies  $\sim 50.8$  to  $\sim 54.0$  at. % based on 100% In and S. This suggests that the average molar ratio between the  $\text{In}_2\text{S}_3$  and  $\text{In}_2\text{O}_3$  is around 2.2 : 1 to 3.6 : 1 in a core-shell particle. To further confirm the formation of the  $\text{In}_2\text{S}_3$  shell, X-ray diffraction traces of both the bare core  $\text{In}_2\text{O}_3$  NCs and the core-shell NPs were comparatively recorded and are presented in Fig. 2. As expected, the pattern of  $\text{In}_2\text{O}_3$  cores shows five peaks at  $2\theta$  values of  $30.56$ ,  $35.46$ ,  $45.62$ ,  $51.05$  and  $60.55$  degrees, corresponding to the  $\text{In}_2\text{O}_3$  lattice planes of (222), (400), (431), (440) and (622), respectively.<sup>21</sup> Compared with this pattern, the core-shell sample shows an additional wide peak centered at  $27.43$  degrees, which is attributed to the (109) diffraction of  $\text{In}_2\text{S}_3$ .<sup>22</sup>

The photoluminescence (PL) spectra of bare  $\text{In}_2\text{O}_3$  NCs and  $\text{In}_2\text{O}_3@ \text{In}_2\text{S}_3$  core-shell NPs suspended in hexane were recorded on a Cary Eclipse Fluorescence Spectrophotometer (Varian) and are presented in Fig. 3. With an excitation wavelength of  $233$  nm, several emission peaks centered at  $422$ ,  $440$ ,  $461$ ,  $484$  and  $533$  nm could be detected from the spectra of both  $\text{In}_2\text{O}_3$  NCs and  $\text{In}_2\text{O}_3@ \text{In}_2\text{S}_3$  NPs. The difference between the spectra of  $\text{In}_2\text{O}_3$  NCs with and without

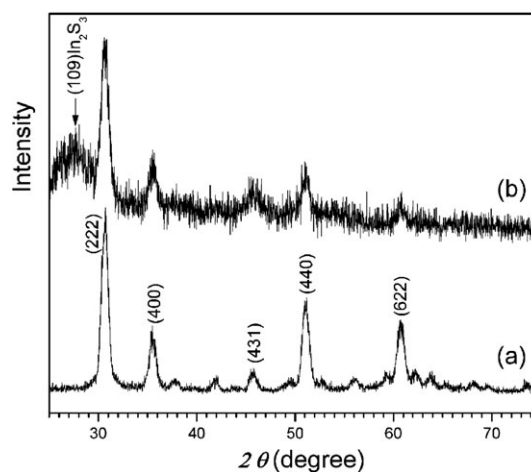


**Fig. 2** X-Ray diffraction patterns of (a)  $\text{In}_2\text{O}_3$  nanocrystals and (b)  $\text{In}_2\text{O}_3@ \text{In}_2\text{S}_3$  core-shell nanoparticles.

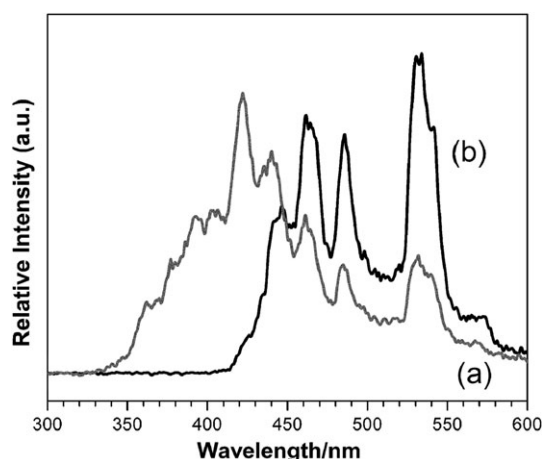


**Fig. 3** Photoluminescence spectra of (a)  $\text{In}_2\text{O}_3$  nanocrystals; and (b)  $\text{In}_2\text{O}_3@ \text{In}_2\text{S}_3$  core-shell nanoparticles suspended in hexane.

$\text{In}_2\text{S}_3$  shell is the changes of the relative intensities at those peaks. For the core-shell NPs, the peak at 422 nm almost vanishes and the relative intensity of the peak at 440 nm apparently decreases, whereas all of other peaks can be determined with relatively enhanced intensities. It is well known that bulk  $\text{In}_2\text{O}_3$  has no PL emission at room temperature. However, many researchers reported the emission of  $\text{In}_2\text{O}_3$  NCs,<sup>10,23–25</sup> nanowires,<sup>26,27</sup> nanofibers,<sup>28</sup> and nanocubes,<sup>29,30</sup> and they were mainly attributed to deeper energy level emissions and oxygen deficiency emissions<sup>29</sup> although the PL emission mechanism of  $\text{In}_2\text{O}_3$  is still ambiguous. In our case, the PL emissions are in the near UV and visible region when excited at the far UV region. The  $\text{In}_2\text{S}_3$  shell does not change the positions of  $\text{In}_2\text{O}_3$  emission but it does alter the relative intensities. Due to the fact that there may be oxygen deficiencies at the interface of the core-shell and the core of wide bandgap  $\text{In}_2\text{O}_3$  surrounded by the narrow bandgap  $\text{In}_2\text{S}_3$ , the energy could be transferred from the conduction band of  $\text{In}_2\text{O}_3$  to the upper energy level of the  $\text{In}_2\text{S}_3$  shell and to the energy level of oxygen deficiency when a sample is excited by a light with wavelength in the far UV region, resulting in a decrease of the near band-edge emission ( $\sim 422$  nm and 440 nm) and an increase of oxygen deficiency emission. We therefore attribute the emission at 422 nm and 440 nm to the near band-edge emission and the other peaks should be related to the oxygen deficiency. In order to correlate the PL changes (which are associated with the  $\text{In}_2\text{S}_3$  shell formation) with various reaction parameters, we examined the PL spectra under different reaction conditions. Several typical PL spectra recorded with different reaction parameters including the amount of reducing agent (superhydride), the reducing time, excess  $\text{CS}_2$  and the sulfidization time, are given in Fig. S2 in ESI.† It seems that the reduction process is a key step compared with the sulfidization for the formation of  $\text{In}_2\text{S}_3$  shells.

In conclusion, we have successfully synthesized  $\text{In}_2\text{O}_3@ \text{In}_2\text{S}_3$  reverse type-I core-shell NPs using our recently developed one-pot reduction method in solution. The existence of the  $\text{In}_2\text{S}_3$  shell is confirmed by HRTEM, EDS and XRD investigations. The TEM images also clearly reveal the partial

reduction of the  $\text{In}_2\text{O}_3$  core on the surface (core diameter “shrinks”) and the formation of the highly crystalline  $\text{In}_2\text{S}_3$  shell. The optical studies suggest that the PL emissions at 422 and 440 nm could be attributed to the near band-edge emission and the other emissions at 461, 484 and 533 nm should be related to the oxygen deficiency. This approach may be able to extend to the syntheses of other sulfide core-shell NPs.

This work was supported by US NSF CAREER program (DMR-0449580/0731382) and State University of New York at Binghamton, USA.

## Notes and references

- R. A. Caruso and M. Antonietti, *Chem. Mater.*, 2001, **13**, 3272–3282.
- F. Caruso, M. Spasova, V. Salgueirino-Maceira and L. M. Liz-Marzan, *Adv. Mater.*, 2001, **13**, 1090–1094.
- Z.-j. Jiang and C.-y. Liu, *J. Phys. Chem. B*, 2003, **107**, 12411–12415.
- H. Sertchook and D. Avnir, *Chem. Mater.*, 2003, **15**, 1690–1694.
- T. Mokari and U. Banin, *Chem. Mater.*, 2003, **15**, 3955–3960.
- J. J. Li, Y. A. Wang, W. Guo, J. C. Keay, T. D. Mishima, M. B. Johnson and X. Peng, *J. Am. Chem. Soc.*, 2003, **125**, 12567–12575.
- D. V. Talapin, R. Koeppel, S. Götzinger, A. Kornowski, J. M. Lupton, A. L. Rogach, O. Benson, J. Feldmann and H. Weller, *Nano Lett.*, 2003, **3**, 1677–1681.
- M. Protière and P. Reiss, *Chem. Commun.*, 2007, 2417–2419.
- X. Zhong, R. Xie, Y. Zhang, T. Basché and W. Knoll, *Chem. Mater.*, 2005, **17**, 4038–4042.
- Q. Liu, W. Lu, A. Ma, J. Tang, J. Lin and J. Fang, *J. Am. Chem. Soc.*, 2005, **127**, 5276–5277.
- P. m. Sirimanne, S. Shiozaki, N. Sonoyama and T. Sakata, *Sol. Energy Mater. Sol. Cells*, 2000, **62**, 247–258.
- K. S. Ramaiah, V. S. Raja, A. K. Bhatnagar, R. D. Tomlinson, R. D. Pilkington, A. E. Hill, S. J. Chang, Y. K. Su and F. S. Juang, *Semicond. Sci. Technol.*, 2000, **15**, 676–683.
- S. A. (Levi), O. Palchik, V. Palchik, M. A. Slifkin, A. M. Weiss and A. Gedanken, *Chem. Mater.*, 2001, **13**, 2195–2200.
- J. Tabernor, P. Christian and P. O'Brien, *J. Mater. Chem.*, 2006, **16**, 2082–2087.
- W.-T. Kim and C.-D. Kim, *J. Appl. Phys.*, 1986, **60**, 2631–2633.
- P. M. Sirimanne, N. Sonoyama and t. Sakata, *Chem. Phys. Lett.*, 2001, **350**, 211–215.
- A. Narayanaswamy, H. Xu, N. Pradhan, M. Kim and X. Peng, *J. Am. Chem. Soc.*, 2006, **128**, 10310–10319.
- Caution: to deal with this hot solution, proper gloves should be worn.
- J.-w. Seo, Y.-w. Jun, S.-w. Park, H. Nah, T. Moon, B. Park, J.-G. Kim, Y. J. Kim and J. Cheon, *Angew. Chem., Int. Ed.*, 2007, **46**, 8828–8831.
- S. Sun and C. B. Murray, *J. Appl. Phys.*, 1999, **85**, 4325–4330.
- JCPDS 06-0416.
- JCPDS 25-0390.
- W. S. Seo, H. H. Jo, K. Lee and J. T. Park, *Adv. Mater.*, 2003, **15**, 795–797.
- A. Murali, A. Barve, V. J. Leppert and S. H. Risbud, *Nano Lett.*, 2001, **1**, 287–289.
- H. Zhou, W. Cai and L. Zhang, *Appl. Phys. Lett.*, 1999, **75**, 495–497.
- H. Cao, X. Qiu, Y. Liang, Q. Zhu and M. Zhao, *Appl. Phys. Lett.*, 2003, **83**, 761–763.
- M. J. Zheng, L. D. Zhang, G. H. Li, X. Y. Zhang and X. F. Wang, *Appl. Phys. Lett.*, 2001, **79**, 839–841.
- C. Liang, G. Meng, Y. Lei, F. Philipp and L. Zhang, *Adv. Mater.*, 2001, **13**, 1330–1333.
- Q. Tang, W. Zhou, W. Zhang, S. Ou, K. Jiang, W. Yu and Y. Qian, *Cryst. Growth Des.*, 2005, **5**, 147–150.
- C. H. Lee, M. Kim, T. Kim, A. Kim, J. Paek, J. W. Lee, S.-Y. Choi, K. Kim, J.-B. Park and K. Lee, *J. Am. Chem. Soc.*, 2006, **128**, 9326–9327.